

Synthesis and Characterization of Pure CoO and Ni-doped CoO-NiO-SiO₂ Nanocomposites Using Sol-Gel Technique

HARISH KUMAR¹, DHARM VEER² and RAMMEHAR SINGH²

¹Department of Chemistry, Chaudhary Devi Lal University, Sirsa (Haryana) -125 055, India

²Department of Physics, Chaudhary Devi Lal University, Sirsa (Haryana) - 125 055, India
harimoudgill@gmail.com

Received 17 September 2017 / Accepted 3 October 2017

Abstract: Co_{1-x}Ni_xO-SiO₂ (x=0.00,0.30) nanocomposites were prepared by using sol-gel technique at room temperature which were further annealed at 400 °C. The powder samples were characterized by XRD, TEM, FTIR and UV-Visible spectroscopy techniques. The lattice parameter of CoO and Co_{0.7}Ni_{0.3}O in SiO₂ supports nanocomposites are a=8.0703 and a=8.2252Å, respectively. The particle size for undoped cobalt oxide and Ni doped cobalt oxide samples at 400 °C, comes out to be 17.50 and 15.53 nm, respectively.

Keywords: Cobalt oxide, Nickel oxide, Nanocomposites, Sol-gel technique, Metal nanoparticles, XRD

Introduction

The transition metal oxides like nickel, copper, manganese, platinum and cobalt are used as electrode materials in various electrochemical processes. Nickel is used as dopant with various transition metals like Zn, Co, Cu *etc.*, to produce better optical, electrical and catalytic materials¹. The compounds formed by the Ni and Co oxides are used as transistor, resistor and capacitors because of their high electrical properties. The nickel and cobalt oxides are widely used in batteries, hard alloy, magnetic, catalyst and electrical materials^{2,3}. Nickel and cobalt oxide shows *p*-type semiconducting behavior similar to intrinsic spinel cobalt oxide⁴. Our interest in nickel cobalt oxide is due to their enormous uses like as electrode material in batteries⁵ in solar cells⁶, a heterogeneous optical recording media⁷, super capacitor⁸, sensors or optical limiters, switches⁹ and in flat panel displays *etc.* The spinel oxide of nickel-cobalt has well documented and established applications in electrochemistry.

Co-NiO is a *p*-type semiconductor having infrared transparent optical properties. Doping of cobalt oxide with nickel produces a significant increase in electrical conductivity without any change in spinel structure. Nickel cations are found to reside in octahedral sites with a valence state of +2 and +3.

Transparent conducting oxides are basically doped metal oxide semiconductor categories into *n*-type and *p*-type. The *p*-type semiconductor oxide material shows lower electrical conductivity than *n*-type materials. NiO and CoO is *p* type semiconductor oxide which can have large number of potential applications. It was found that mixed oxides of nickel and cobalt are more conductive in comparison with either of the two end members^{10,11}. Windisch *et al.*, determined the carrier to be *p*-type and reported that Ni³⁺ has a role in conductivity such that the mechanism of conduction is a charge transfer, between resident divalent and trivalent cation¹²⁻¹⁴. Therefore, there is an increase demand of conducting oxides with optical transparency at longer wavelength. Nickel cobalt oxide is a spinel compound which can provide transitivity from visible wavelength 12 micrometer in IR region¹⁵. This binary oxide system has application such as electro catalyst for anodic oxygen evolution, inorganic and organic electro synthesis, super capacitors or infrared transparent conducting electrodes for flat panel displays¹⁶, sensors or optical limiters and switches.

In continuation to our earlier study^{17,18}, here we have synthesized CoO-NiO-SiO₂ nanocomposites by sol-gel method and structural and optical characterization was carried out by using techniques like x-ray diffraction (XRD), TEM, FTIR and UV-Visible spectroscopy.

Experimental

Stoichiometric amounts of NiCl₂ and CoCl₂ were dissolved separately in a beaker in 50 mL of double distilled water and mix it with the help of magnetic stirrer for 15 minute (Solution A). Then dilute nitric acid solution was added drop by drop in order to make pH between 1-2 in solution A. Nitric acid acts as a catalyst to alter the rate of hydrolysis and condensation. Another solution B was prepared by mixing TEOS and ethanol in 1:4 molar ratio. Now solution A was added drop wise to solution B by gentle stirring on magnetic stirrer over a period of 6.0 hours maintained at a constant temperature of 70 °C. Resulting solution was dried in oven for 24 hours at 100 °C. The gel appeared was further kept in oven for aging for 15 days at 100 °C. The aging process allows further shrinkage and stiffening of the gel. Annealing of samples were carried out for 4 hours at a constant temperature of 400 °C.

Characterization techniques

Structural and optical properties of Co-NiO nanoparticles were determined by x-ray diffraction (XRD) (Panalytical's X'pert Pro using Cu-Kα 1, λ=0.151406 nm radiations), transmission electron microscopy (TEM) (Tecnai 200KV Fei Electron Optics λ=35 nm), infra-red spectroscopy (FTIR) (SHAMDZU, IR Affinity-1) in the wavelength range of 400-4000 cm⁻¹ and UV-Visible spectroscopy (Nanodrop-2003, Thermo-scientific company) in the wavelength range of 200-800 nm.

Results and Discussion

X-Ray diffraction analysis

Figure 1 shows that diffraction pattern of Co_{1-x}Ni_xO (x=0.0, 0.3) nanocomposites characterized by XRD. The diffraction pattern of both samples can be indexed to the face centered cubic structure of CoO agreed with the reported papers¹⁹⁻²¹. No additional peaks attributes to secondary phases such as Ni metal and its oxides are obtained for x=0.30, which indicates that the structure is not disturbed by the Ni substitution. The average crystallite size is determined by relationship between crystal grain size and X-Ray line broadening by the Debye Scherrer's formula:

$$d = \frac{k\lambda}{\beta \cos \theta} \quad (1)$$

Where, k is polarization (shape) factor, λ wavelength of light ($\lambda=1.542 \text{ \AA}$) ($\text{CuK}\alpha$), β is the full width at half maximum (FWHM) of the line and θ is the diffraction angle.

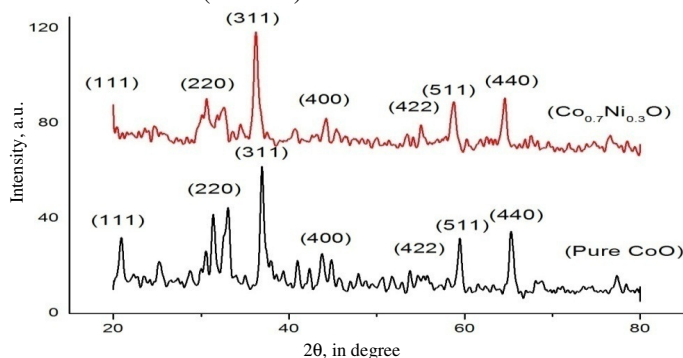


Figure 1. X-ray diffraction pattern of (a) Pure CoO nanoparticle and (b) $\text{Co}_{0.7}\text{Ni}_{0.3}\text{O}$ nanocomposites

Average particle size of cobalt oxide and Ni-Cobalt oxide samples at 400°C was found to be 17.50 and 15.53 nm, respectively. The lattice parameters (a) of the samples are calculated using the formula:

$$\frac{1}{d^2} = \left(\frac{h^2 + k^2 + l^2}{a^2} \right) \quad (2)$$

The lattice parameter of CoO and $\text{Co}_{0.7}\text{Ni}_{0.3}\text{O}$ powder samples are $a=8.0703$ and $a=8.2252 \text{ \AA}$, respectively. The lattice parameters of $\text{Co}_{0.7}\text{Ni}_{0.3}\text{O}$ are found to be increased slightly due to the larger ionic radii of Ni^{2+} (0.68 \AA) than that of Co^{2+} (0.65 \AA) in the tetrahedral coordination, which reveals that the mixing of Ni does not change the CoO structure and hence Ni^{2+} substitutes Co^{2+} into the crystal lattice.

The distance between magnetic ions (hopping length) in A site (tetrahedral) and B site (octahedral) were calculated using the relations $d_A = 0.25a\sqrt{3}$ and $d_B = 0.25a\sqrt{2}$. The calculated values of hopping length for tetrahedral site (d_A) and octahedral site (d_B) of different compositions were tabulated in Tables 1-3.

Volume of the unit cell was calculated by using the formula $V = a^3$ in \AA^3 Where, ' a ' is lattice parameter. Volume of unit cell was found to be increase with Ni doping, as it depend on lattice parameter which was found to be increased with Ni doping²².

Table 1. Calculated value of lattice parameter and d -values from different planes for pure cobalt oxide nanoparticles

Angle(2θ)	d -values	$\langle h, k, l \rangle$ planes	$a(\text{\AA})$
20.98	4.2382	111	7.3407
32.98	2.7158	220	7.6814
36.94	2.4333	311	8.0703
43.86	2.0641	400	8.2564
55.32	1.6606	422	8.1352
59.48	1.5540	511	8.0748
65.26	1.4296	440	8.0870

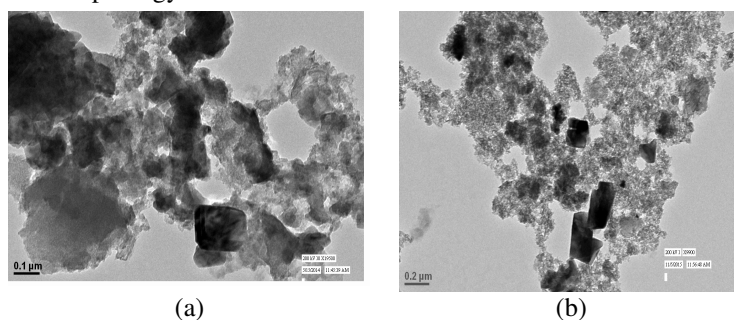
Table 2. Calculated value of lattice parameter and d -values from different planes for $\text{Co}_{0.70}\text{Ni}_{0.30}\text{O}$ Nanocomposites

Angle(2θ)	d -values	$\langle h, k, l \rangle$ planes	$a(\text{\AA})$
20.34	4.3659	111	7.5619
32.58	2.7483	220	7.7733
36.22	2.4800	311	8.2252
44.36	2.0420	400	8.1680
55.10	1.6667	422	8.1651
58.82	1.5693	511	8.1543
65.60	1.4230	440	8.0497

Table 3. Values of crystallite size, lattice parameter (a), lattice strain (ϵ), x-ray density and hopping length for A-Site (d_A) and B-Site (d_B) for Pure Co oxide nanoparticles and Ni doped Co Oxide ($\text{Co}_{0.70}\text{Ni}_{0.30}\text{O}$) Nanocomposites

Sample	Particle size, nm	Lattice parameter	Lattice strain	Unit Cell volume(a.u)	A-Site (d_A)	B-Site (d_B)
CoO	17.50	8.0703	0.0065	525.616	3.4945	2.8532
$\text{Co}_{0.70}\text{Ni}_{0.30}\text{O}$	15.53	8.2252	0.0075	556.466	3.5616	3.0130

Figure 2 shows the TEM images of as prepared nanocrystalline CoO and Ni/CoO ($\text{Co}_{0.7}\text{Ni}_{0.3}\text{O}$) powders. From the Figure 2, it is clear that the agglomeration of nanoparticles takes place and morphology seems to be almost cubical.

**Figure 2.** TEM micrographs of (a) Pure CoO nanoparticles (b) $\text{Co}_{0.70}\text{Ni}_{0.30}\text{O}$ nanocomposites.

The formation of face centered cubic structure in pure and nanocomposite ($\text{Co}_{0.7}\text{Ni}_{0.3}\text{O}$) nanocrystalline powders is further confirmed by FTIR spectra as shown in Figure 3. The absorption bands around 3386 and 3419 cm^{-1} are may be due to presence of coordinated/entrapped water. The absorption bands around 1614 and 1061 cm^{-1} are may be due to carboxylate ion. The absorption bands around 661 cm^{-1} corresponds to bending modes of vibration of cobalt and the absorption band around 575 cm^{-1} corresponds to bending vibration of Nickel oxides²³.

The optical absorption band of $\text{Co}_{1-x}\text{Ni}_x\text{O}$ ($x=0.0, 0.3$) samples by UV-Visible spectrometer in the range of 200 to 800 nm were shown in Figure 4. The wavelength of absorption edges is determined by the extrapolation of the linear part to the x-axis. The absorption edges of nanocrystalline pure CoO and $\text{Co}_{0.7}\text{Ni}_{0.3}\text{O}$ are 220 and 233 nm , respectively. It indicates that a red shift of the band edge can be observed on addition of nickel nanoparticles. The energy band gap values are estimated using the relationship,

$$(\alpha h\nu)^n = A(h\nu - E_g) \quad (3)$$

Where, α is absorption coefficient, $h\nu$ the photon energy, A is a constant characteristics to the material and n is 2 for direct band gap material and $\frac{1}{2}$ for an indirect band gap material. According to the equation, the optical band gap for the absorption peak can be obtained by extrapolating the linear portion of the $(\alpha h\nu)^n$ versus $h\nu$ curve to zero. The energy band for absorption edges of nanocrystalline pure CoO and $\text{Co}_{0.7}\text{Ni}_{0.3}\text{O}$ at 220 and 233 nm was found to be 5.63 and 5.32 eV, respectively.

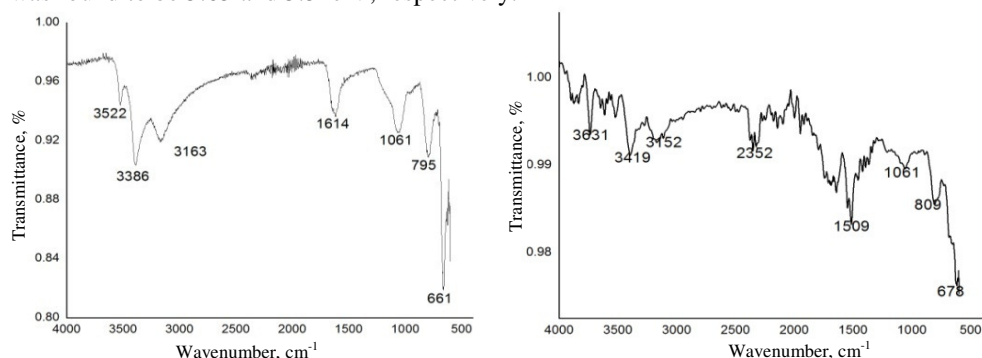


Figure 3. FTIR spectra of (a) Pure CoO nanoparticle (b) $\text{Co}_{0.7}\text{Ni}_{0.3}\text{O}$ nanocomposites

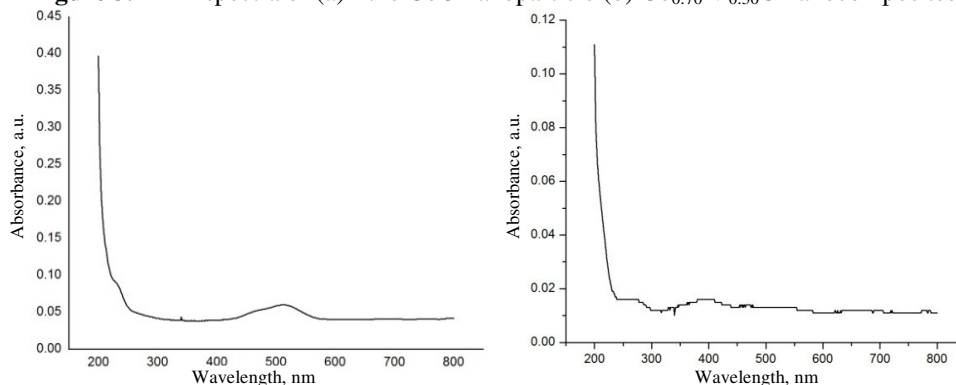


Figure 4. UV-Visible spectra of (a) Pure CoO (b) $\text{Co}_{0.7}\text{Ni}_{0.3}\text{O}$ nanocomposites

Conclusion

Co-NiO nanocomposites were synthesized by sol-gel technique. Characterization of nanoparticles and nanocomposites were carried out using XRD, TEM, FTIR and UV-Visible spectroscopic techniques. Average particle size of CoO and Co-NiO nanocomposite was found to be 17.50 and 15.53 nm, respectively using XRD technique. The energy band gap of CoO and Co/NiO were found to be 5.63 and 5.32 eV, respectively. The characteristics peaks at 678.0, 809.0 cm^{-1} in the finger print region corresponds to CoO and NiO stretching vibrations in CO-NiO nanocomposites. Average particle size, lattice parameters, inter planar spacing and dislocation density of CoO and Co-NiO nanocomposites were also calculated from x-ray diffraction study.

References

1. Chauhan R, Ashvani K and Chaudhary R P, *Res Chem Int.*, 2012, **38**(7), 1483-1493; DOI:10.1007/s11164-011-0478-5

2. Chakrabarty S and Chatterjee K, *J Phys Sci.*, 2009, **13**, 245-250.
3. Chang H and Su H T, *Rev Adv Mater Sci.*, 2008, **18**, 667-675.
4. Tareen J A K, Malecki A, Doumerc J P, Launay J C, Dordor P, Pochard M and Hagenmuller P, *Mater Res Bull.*, 1984, **19(8)**, 989-997; DOI:10.1016/0025-5408(84)90212-5
5. Liu Z L, Yu A S and Le J Y, *J Power Sources*, 1999, **81-82**, 416-419; DOI:10.1016/S0378-7753(99)00221-9
6. Park S, Keszler D A, Valencia M M, Hoffman R L, Bender J P and Wager J F, *Appl Phys Lett.*, 2002, **80**, 4393; DOI:10.1063/1.1485133
7. Iida A and Nishikawa R, *Jap J Appl Phys Part 1*, 1994, **33(7A)**, 3952.
8. Hu C C and Cheng C Y, *Electrochem Solid State Lett.*, 2002, **5(3)**, A43-A46; DOI:10.1149/1.1448184
9. Goodwin J S H, Holloway S P, McGuire P, Buvkley L J, Cozzens R F, Robert W S and Gregory J E, *Actuators Devices*, 2000, **3987**, 225; DOI:10.1117/12.387781
10. Domnisky K, Rose A, Gover W H and Exarhos G J, *Mater Sci Eng B-Solid.*, 2000, **76(2)**, 116-121; DOI:10.1016/S0921-5107(00)00425-6
11. Marco J F, Gancedo J R, Ortiz J and Gautier J L, *Appl Surf Sci.*, 2004, **227(1-4)**, 175-186; DOI:10.1016/j.apsusc.2003.11.065
12. Exarhos G J, Rose A and Windisch C F, *Thin Solid Films*, 1997, **308-309**, 56-62; DOI:10.1016/S0040-6090(97)00536-1
13. Windisch C F Jr, Ferris K F and Exarhos G J, *J Vac Sci Technol A*, 2001, **19**, 1647; DOI:10.1116/1.1351799
14. Windisch C F Jr., Exarhos G J and Sharma S K, *J Appl Phys.*, 2002, **92**, 5572; DOI:10.1063/1.1509838
15. Haenen J, Visscher W and Barendrecht E, *J Electronal Chem.*, 1986, **208(2)**, 323-341; DOI:10.1016/0022-0728(86)80541-1
16. Roginskaya Y E, Morozova O V, Lubnin E N, Ulitina Y E, Lopukhova G V and Trasatti S, *Langmuir*, 1997, **13(17)**, 4621-4627; DOI:10.1021/la9609128
17. Kumar H, Dixit R and Dharm Veer, *Asian J Chem.*, 2017, **29(11)**, 2391-2395; DOI:10.14233/ajchem.2017.20690
18. Kumar H and Manisha K, *Asian J Pharm Clin Res.*, 2017, **10(9)**, 206-209; DOI:10.22159/ajpcr.2017.v10i9.19459
19. Guoxiu W, Xiaoping S, Josip H and Bei W, *J Phys Chem C*, 2009, **113(11)**, 4357-4361; DOI:10.1021/jp8106149
20. Iacomi F, Calin G, Scarlat C and Irimia M, Dorofteia C, Dobromira M, Rusua G G, Iftimiec N and Sandud A V, *Thin Solid Films*, 2011, **520(1)**, 651-655; DOI:10.1016/j.tsf.2011.08.067
21. Nisha J, Tharayil R, Raveendran and Alexander V V, *Mater Sci Res India*, 2007, **4**, 69.
22. Gaffoor A and Ravinder D, *Int J Eng Res Appl.*, 2014, **4(4)**, 73-79.
23. Nisha J, Thaeayil R, Raveendran, Alexander V V and Chithra P G, *Indian J Engg Mat Sci.*, 2008, **15**, 489.